Am J Transl Res 2024;16(11):6528-6539
www.ajtr.org /ISSN:1943-8141/AJTR0158645

Original Article

Exosomal miRNA-let-7i-5p from bone marrow mesenchymal stem cells protects against myocardial infarction by inhibiting myocardial apoptosis

Fei You[1], Yibo Shen[1,2], Yuanyuan Hao[1]

[1]*Department of Cardiology, Xi'an Central Hospital, No. 161 Xiwu Road, Xincheng District, Xi'an 710004, Shaanxi, China;* [2]*School of Medicine, Yan'an University, No. 580 Shengdi Road, Baota District, Yan'an 716000, Shaanxi, China*

Received June 22, 2024; Accepted October 21, 2024; Epub November 15, 2024; Published November 30, 2024

Abstract: Objectives: To elucidate the regulatory effect of exosomes secreted by bone marrow mesenchymal stem cells (BMSCs-exosomes) on cardiomyocyte apoptosis through miRNA-let-7i-5p in myocardial infarction. Methods: BMSCs-exosomes were extracted, and their morphology and size distribution were analyzed using transmission electron microscope. Expression of exosome surface markers was determined by western blot. H9C2 cells were randomly assigned into five groups, namely control, OGD, OGD+exos, OGD+exos+miR-let-7i-5p inhibitor and OGD+exos+miR-let-7i-5p inhibitor NC. Hypoxic cardiomyocytes were induced using glucose-free Dulbecco's Modified Eagle Medium (DMEM). Mice were randomly assigned into sham, myocardial infarction (MI), MI+exos, MI+exos+miR-let-7i-5p inhibitor and MI+exos+miR-let-7i-5p inhibitor NC groups. MI model was established by ligation of the left anterior descending (LAD) coronary artery. Subsequently, BMSCs-exosomes or BMSCs-exosomes transfected with miRNA-let-7i-5p inhibitor were incubated with hypoxia cardiomyocytes or injected into the MI mouse model. Cell survival was accessed by CCK-8 assay. Cardiomyocyte apoptosis was accessed with V-FITC/PI and TUNEL. Heart function of MI mice was evaluated by echocardiography. Myocardial infarct size was calculated through TTC staining. Relative miRNA-let-7i-5p expression level was determined by RT-qPCR. Expression of apoptosis-related proteins in myocardial tissue were detected by western blot. Results: Exosomes secreted from BMSCs were successfully extracted. In H9C2 cells, miRNA-let-7i-5p expression was significantly upregulated, cell survival rate was increased, and the apoptosis rate was decreased after incubation with BMSCs-exosomes. In MI mice, injection of BMSCs-exosomes markedly upregulated miRNA-let-7i-5p level, reduced infarct size, improved cardiac function, and decreased apoptotic rate. BMSCs-exosomes treatment downregulated Bax and upregulated Bcl-2 protein expression. These effects were reversed by transfection with the miRNA-let-7i-5p inhibitor. Conclusions: BMSCs-exosomes inhibit myocardial apoptosis, attenuate MI progression, and protect against myocardial infarction both *in vivo* and *in vitro* through miRNA-let-7i-5p.

Keywords: Exosomes, microRNA-let-7i-5p, myocardial infarction, myocardial apoptosis

Introduction

Despite significant improvements in global health in recent years, cardiovascular diseases (CVDs) remain a leading cause of mortality and disability worldwide [1]. From the Global Burden of Disease (GBD) 2019 Study, CVDs affected around 523 million individuals globally, with around 18.6 million deaths attributed to CVDs in 2019 [2]. Among these, myocardial infarction (MI) accounts for a large proportion, posing a serious threat to human health and placing a substantial economic burden on patients. Rapid and effective treatment for MI is of great significance to improve the global healthcare outcomes. Therefore, in-depth research into the pathogenesis of MI is essential to identify effective treatment strategies that promote myocardial repair.

In recent years, exosomes (exos) have been found to play a crucial role in both the physiologic and pathophysiologic processes of the cardiovascular system, particularly in the development of myocardial infarction [3]. Bone marrow mesenchymal stem cells (BMSCs) are con-

https://doi.org/10.62347/VXND1945

sidered ideal candidates for exosome production due to their strong paracrine effect, easy culture, high proliferative rate, and long-term survival [4]. Exosomes are vesicles with an average diameter of 100 nm, generated by the direct outward budding of the plasma membrane. They carry a range of biologically active substances, such as protein, lipids, mRNA, microRNA, mtDNA, enabling them to convey disease-related information [5]. Cell-cell communication via miRNAs is particularly important in disease progression. Accumulating evidence shows that miRNAs regulate many biologic processes, including cell proliferation, differentiation, apoptosis, autophagy, mitochondrial metabolism, angiogenesis, neoplasia, and hematopoiesis [6-9]. Thomas and Liu et al. found that let-7i-5p plays a role in inflammation, cell proliferation, and tumor growth [10, 11]. MiRNA-let-7i-5p has been reported to mediate hypoxic injury of cardiomyocytes, playing a decisive role in MI [12]. Previous studies have shown that miRNA-let-7i-5p exhibits anti-inflammatory, anti-oxidation and anti-apoptosis effects. Based on these findings, we speculated that BMSCs-exosomes could inhibit cardiomyocyte apoptosis and improve cardiac function through miRNA-let-7i-5p under hypoxic state. Therefore, we established an *in vivo* mouse model of MI and an *in vitro* model of cardiomyocyte hypoxia, extracting BMSCs-exosomes and injecting them into the infarcted myocardium along miRNA-let-7i-5p inhibitors. We aim to elucidate the regulatory effect of BMSCs-exosomes on cardiomyocyte apoptosis through miRNA-let-7i-5p after MI, and explore a possible protective role in myocardial infarction.

Materials and methods

Extraction, identification and analysis of BMSCs-exosomes

BMSCs were isolated from SD mice. Bone marrow was flushed from the tibia and femur under aseptic conditions and collected. The cell suspension was seeded into dishes containing complete Dulbecco's Modified Eagle Medium (DMEM). After centrifugation at 2000×g for 5 min, the cell density was adjusted in fresh complete DMEM medium. Then, the medium was replaced with fresh DMEM every 2 days, and the cells were cultured until the third passage. Upon reaching 70% confluence, the cells were transferred to chemically defined and protein-free medium (CDPF) for continued incubation for 48 h at 37°C. BMSCs were collected for further culture.

Exosomes were isolated from the BMSCs culture medium through a series of centrifugation and filtration steps at 4°C. Briefly, the conditioned medium was centrifuged at 2000×g for 15 min to remove cells and cellular debris, followed by further centrifugation at 10000×g for 30 min to remove subcellular structures. Finally, exosomes were collected by ultracentrifugation for 70 min.

The extracted exosomes were suspended in phosphate-buffered saline (PBS) and stored at -80°C. To further verify the extracted exosomes, transmission electron microscope (TEM) (JEM-1400, JEOL Ltd., Japan) was used to detect their morphology and size distribution. Additionally, western blot was performed to detect the levels of exosome surface markers CD63 (1:1000, Abcam, California, USA), CD81 (1:1000, Abcam, California, USA) and TSG101 (1:1000, Abcam, California, USA). The protein content of the exosome suspension was quantified using the bicinchoninic acid (BCA) assay (Beyotime, P0010, Beijing, China), and normalized to a total protein content of 1.1 mg/ml.

Cell culture

H9C2 cells were cultured in glucose-high DMEM dishes (Thermo Scientific, San Jose, CA, USA) containing 10% fetal bovine serum (Gibco, California, USA). The cells were maintained in a 37°C, 5% CO_2 incubator, and culture medium was routinely replaced. Once the cells reached confluence, they were subcultured using 0.4% trypsin digestion.

Exosome labeling and uptake

Laser confocal microscopy was used to detect the uptake of BMSCs-exosomes by H9C2 cells. Briefly, H9C2 cells were digested and seeded in confocal laser dishes for 3 hours, after which the medium was replaced, and the cells were co-cultured with BMSCs-exosomes for 24 hours. CD81 and CTnI antibodies were added overnight. The next day, the cells were stained with DAPI for 15 min in the dark. Laser confocal microscopy showed that the BMSCs-exosomes were stained red by CD81 antibodies, the nuclei

of H9C2 cells were stained blue by DAPI, and the cytoplasm of H9C2 cells was stained green by CTnI antibodies.

Hypoxic treatment

For establishing the hypoxic conditions, H9C2 cells were cultured in glucose-free DMEM dishes (Thermo Scientific, San Jose, CA, USA) in an anaerobic chamber (1% O_2, 5% CO_2) at 37°C for the indicated hours to induce hypoxic ischemic injury. Cells were treated with exosomes or exosomes transfected with miRNA-let-7i-5p inhibitors 6 h after oxygen and glucose deprivation (OGD) treatment. The cells were divided into five groups: control, OGD, OGD+exos, OGD+exos+miR-let-7i-5p inhibitor and OGD+exos+miR-let-7i-5p inhibitor NC.

CCK-8 assay

Cell survival was assessed by a Cell Counting Kit-8 assay (CCK-8, Dojindo Molecular Technologies, Gaithersburg, MD, USA). Briefly, H9C2 cells were seeded into 96-well plates with 5000 cells per well, with 5 replicate wells for each group. Different doses of BMSCs-exosomes (0, 5, 10, 20, 50 ug/mL) were added to the H9C2 cells. CCK-8 solutions (Dojindo, Kumamoto, Japan) were added and incubated at 37°C for 1 h. The absorbance (A) value of each well was measured at 490 nm using a Microplate Reader (Bio-Rad, Hercules, CA, USA). This experiment was independently repeated three times.

Cell transfection

MiRNA-let-7i-5p mimic, miRNA-let-7i-5p mimic NC, miRNA-let-7i-5p inhibitor and miRNA-let-7i-5p inhibitor NC were provided by RiboBio (Guangzhou, China). For transfection, H9C2 cells were pre-seeded in a 6-well plate with 2 mL serum-free DMEM. MiRNA-let-7i-5p mimic, miRNA-let-7i-5p mimic NC, miRNA-let-7i-5p inhibitor, miRNA-let-7i-5p inhibitor NC and FAM control were each added to 50 uL of serum-free DMEM medium. Meanwhile, 5 uL of Lipofectamine 2000 transfection reagent (Thermo Fisher Scientific, Waltham, MA, USA) was mixed with 250 uL of serum-free DMEM for 5 min. The above two solutions were mixed in a ratio of 1:1 and then transfected at room temperature for 24 h.

Flow cytometry

Cell apoptosis rate was determined using commercial Annexin V fluorescein isothiocyanate (V-FITC)/propidium iodide (PI) apoptosis detection kit (Sigma-Aldrich, St. Louis, MO, USA) through flow cytometry. In brief, H9C2 cells (1×10^5) in 12-well plate were trypsinized, washed with cold PBS, and harvested. The cells were then double-stained with Annexin V-FITC and PI in the dark. Then, the apoptotic was analyzed by flow cytometry (Becton-Dickinson, Franklin Lakes, NJ, USA), where the FITC+/PI- fraction and FITC+/PI+ fraction represented apoptotic cells (early and late apoptosis, respectively). Apoptosis rate was calculated as the percentage of apoptotic cells.

Mice model of myocardial infarction

Animal experiments were conducted using 6-8-week-old C57B/6 male mice purchased from the Experimental Animal Center of Xi'an Jiaotong University. All animal procedures were performed in accordance with the guidelines for the Care and Use of Laboratory Animals of the National Institutes of Health. MI model was established on 8-week male C57BL/6 mice. Mice were anaesthetized by isoflurane inhalation (2.5%) and ventilated using a rodent ventilator. Thoracotomy was performed at the 4th intercostal space to expose the heart and left anterior descending (LAD) coronary artery. LAD was ligated with a 6-0 suture. Continuous elevation of S-T segment confirmed the successful establishment of MI model. Immediately after ligation, the peri-infarct myocardial region was injected at three different points with a total of 10 uL of exosomes or exosomes transfected with miRNA-let-7i-5p inhibitors. In the MI group, mice were injected with 10 uL PBS alone. In the sham group, the LAD was not ligated. The animals were divided into five groups accordingly: sham, MI, MI+exos, MI+exos+miR-let-7i-5p inhibitor and MI+exos+miR-let-7i-5p inhibitor NC. At the end of modeling, mice were sacrificed by decapittal under pentobarbital sodium anesthesia at 24 hours, 3 days, and 28 days, and hearts were collected.

Echocardiography

Echocardiography was performed before and 1 week after operation to monitor cardiac function. Transthoracic echocardiography was performed according to previously reported classical method [13, 14]. After anesthesia, the mice were subjected to two-dimensional M-mode transthoracic echocardiography to evaluate cardiac function. The relevant parameters,

including left ventricular ejection fraction (LVEF) and left ventricular shortening fraction (LVFS), were recorded.

TTC staining

Mice were sacrificed 24 h after MI and hearts were harvested for sectioning. Mice were anesthetized by intraperitoneal injection of 1.8% sodium pentobarbital (60 mg/kg) and sacrificed, and the hearts were quickly removed and placed on dry ice. Frozen hearts from each group were sliced into 2 mm thick sections, which were then incubated in 1% triphenylterazolium chloride (TTC) at 37°C for 20 min in the dark. After staining, the sections were fixed and photographed to calculate the myocardial infarction area. Infarcted areas appeared pale, while non-infarcted areas were in deep red. Infarct size was calculated using the Image J (National Institutes of Health, USA) as the ratio of infarct size to the total heart size.

TUNEL assay

Apoptosis in mice myocardial tissue sections and in H9C2 cells were determined using a TUNEL assay according to the instructions provided by the In Situ Cell Apoptosis Detection Kit (Servicebio, Wuhan, China). Briefly, three days after induction of MI, mice were sacrificed by decapittal after anesthesia, and hearts were rapidly removed. The hearts were rinsed in ice-cold PBS to remove blood. Myocardial tissue from the ischemic area was collected for experiments. After various treatments, the myocardial cells were incubated with fresh TUNEL solution for 1 h at 37°C in the dark. The cells were then re-stained with 100 ng/ml DAPI for 10 min. Phase images, TUNEL signals, and DAPI signals were observed using fluorescent microscopy. For each sample, five randomly selected fields were observed for counting TUNEL positive cells (green) and DAPI stained nucleus (blue). Cell apoptosis was quantified using Image J software to calculate the percentage of TUNEL-positive cells.

Real-time quantitative polymerase chain reaction (RT-qPCR)

Four weeks post-operation, the mice were sacrificed after anesthesia, and the hearts of mice were taken, and the heart chambers were repeatedly washed with PBS. The myocardial tissue was collected from the ischemic area. MiRNA from both the *in vitro* and *vivo* experimental groups was extracted using Trizol reagent (Invitrogen, USA). The extracted miRNA was analyzed using the miRcute Enhanced miRNA Fluorescence Quantitative Detection Kit. PCR was carried out using a fluorescence real-time quantitative PCR instrument (Roche, Switzerland) under the following conditions: pre-denaturation for 3 min at 95°C, followed by 38 cycles of denaturation for 15 s at 95°C, annealing for 60 s at 60°C, and extension for 40 s at 72°C. Relative let-7i-5p expression level was determined using the $2^{-\Delta\Delta}$Ct method, with normalization to U6 RNA levels.

Western blot

The expression of apoptosis-related proteins was measured using western blot following total protein extraction. Protein from both the *in vitro* and *in vivo* experimental groups was extracted using a Cells Protein Extraction Kit (Jiangsu Biyuntian Company, China). Protein concentrations of each sample were determined using a BCA protein Concentration Determination Kit (Jiangsu Biyuntian Company, China). Then, 20 ug of protein sample was used for standard western blot procedures. Primary antibodies targeting Bax and Bcl-2 (1:1000, Abcam, USA), as well as the secondary antibody targeting rabbit IgG (1:5000, Servicebio, Wuhan, China) were used. Finally, the signal was detected by enhanced chemiluminescence using a Bio-rad western blotting imaging system (Bio-rad, Hercules, USA). The relative expression of proteins was normalized to β-actin.

Statistical analysis

Data were expressed as Mean ± SD. Statistical Product and Service Solutions (SPSS) 21.0 statistical software (IBM, Armonk, NY, USA) was used for data processing and analysis. GraphPad Prism 9 (GraphPad Prism, USA) was used for figure editing. A t-test was used to compare the mean values of two independent samples, while one-way analysis of variance (ANOVA) was employed for multiple group comparisons. A $P<0.05$ was considered statistically significant.

Results

Extraction and identification of BMSCs-exosomes

Exosomes were isolated from the BMSCs-conditioned medium and characterized by TEM

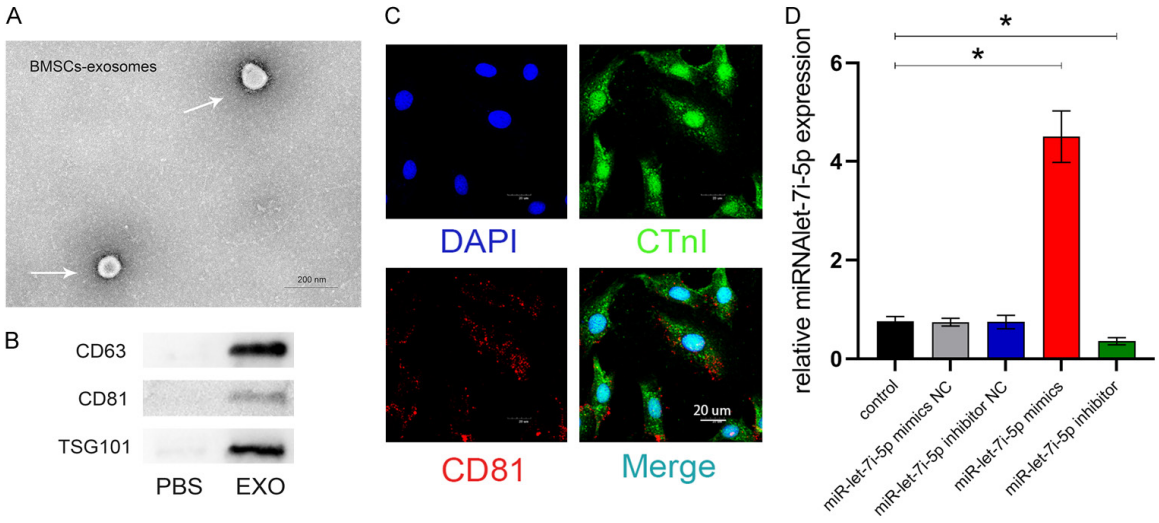

Figure 1. Identification of BMSCs-exosomes and uptake of BMSCs-exosomes by H9C2 cells. A. Transmission electron micrographs of exosomes. Scale bar-200 nm. B. Western blot analyses of exosome surface markers, CD63, CD81 and TSG101. C. The uptake of BMSCs-exosomes by H9C2 cells, and the localization of labeled BMSCs-exosomes (red) in H9C2 cells cytoplasm (green) and the nucleus (blue). Scale bar-20 um. D. Relative expression of miR-let-7i-5p in H9C2 cells transfected with miR-let-7i-5p mimic, miR-let-7i-5p mimic NC, miR-let-7i-5p inhibitor, or miR-let-7i-5p inhibitor NC (n=6/group). *P<0.05. Data are presented as mean ± SEM. BMSCs: Bone marrow mesenchymal stem cells.

and protein marker expression. The morphologies of exosomes under TEM are shown in **Figure 1A**. The diameter of the exosomes ranged from 30 to 150 nm, consistent with previously reported sizes [15]. We randomly measured the diameters of 20 BMSCs-exosomes, and they had an average diameter of 97 nm. The exosomes appeared as round vesicles with a complete structure, light-stained center, and clear margin. Western blot analysis of lysed exosomes confirmed the presence of exosome markers, CD63, CD81 and TSG101 (**Figure 1B**). To further understand how BMSCs-exosomes interact with H9C2 cells, H9C2 cells were co-cultured with BMSCs-exosomes. Laser confocal microscope revealed a large amount of punctate red fluorescence (BMSCs-exosomes) within the cytoplasm of H9C2 cells (green fluorescence), while the nuclei of H9C2 cells were stained blue (**Figure 1C**). These results indicated that BMSCs-exosomes were successfully incorporated into H9C2 after 24 hours of incubation.

To further explore the roles of miRNA-let-7i-5p mimic and miRNA-let-7i-5p inhibitor in H9C2 cells, cell transfection was performed. H9C2 cells were transfected with miRNA-let-7i-5p mimic, miRNA-let-7i-5p mimic NC, miRNA-let-7i-5p inhibitor or miRNA-let-7i-5p inhibitor NC before hypoxia treatment, and the transfection efficiency was evaluated. As demonstrated in **Figure 1D**, RT-qPCR demonstrated that transfection with miRNA-let-7i-5p inhibitor efficiently reduced the level of miRNA-let-7i-5p in H9C2 compared with the control (all P<0.05). Conversely, transfection with miRNA-let-7i-5p mimic efficiently increased the level of miRNA-let-7i-5p in H9C2 compared with other groups (all P<0.05). These results indicated successful transfection, laying the foundation for further research.

Effect of exosome concentration and exosomes-miRNA-let-7i-5p on H9C2 cell survival

Different concentrations of BMSCs-exosomes were added to H9C2 cells treated with OGD. The optical density (OD) measurements showed that the concentration of BMSCs-exosomes was positively correlated with the cell survival rate. H9C2 cells treated with 50 μg/ml of BMSCs-exosomes showed the best survival rate, and the cells in 0 μg/ml were the lowest. Additionally, the cell survival rate in 5 μg/ml BMSCs-exosome group was significantly higher than that of the 0 ug/ml group (P<0.05, **Figure 2A**).

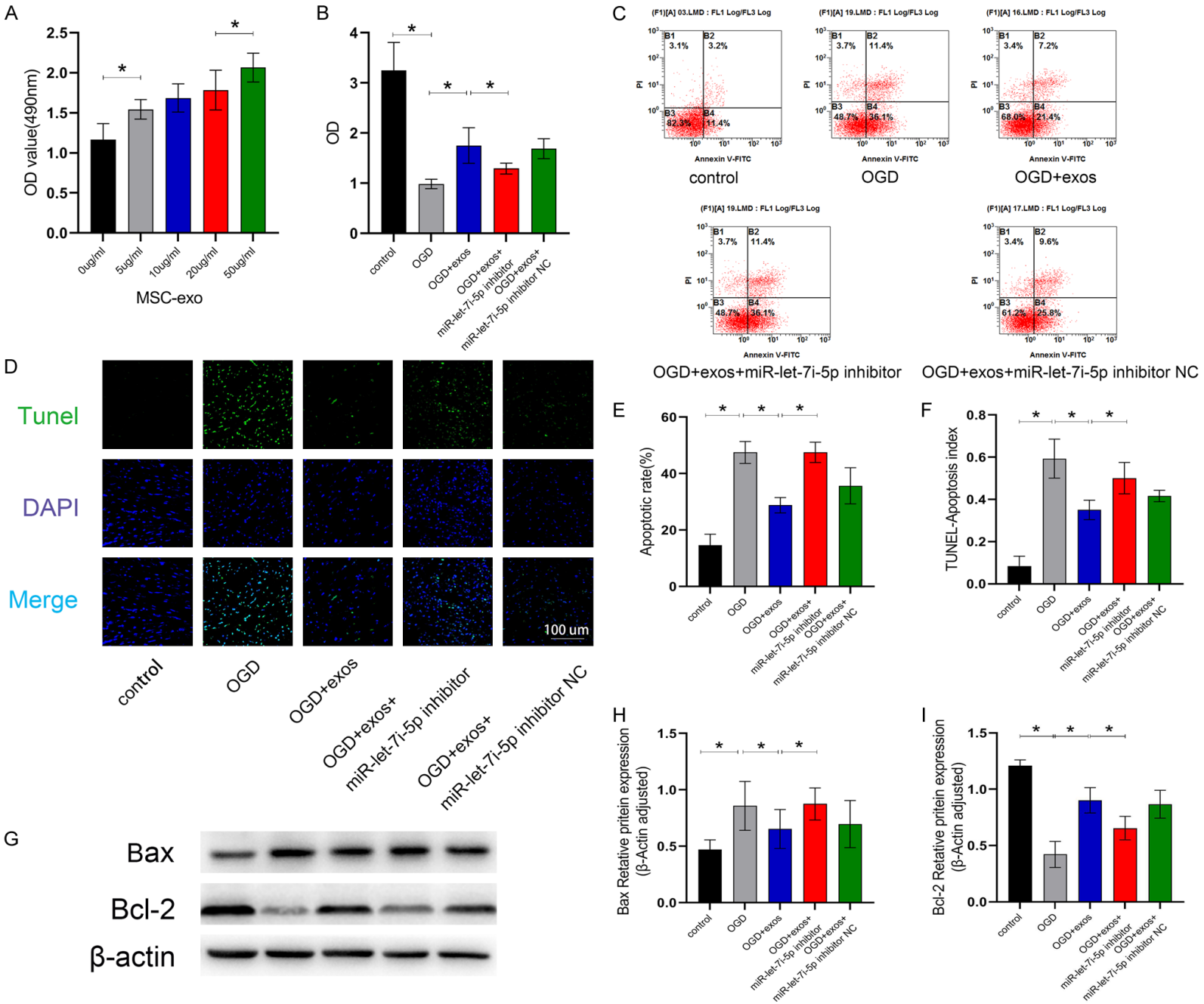
A
OD value(490nm)
0ug/ml
5ug/ml
10ug/ml
20ug/ml
50ug/ml
MSC-exo
B
OD
control
OGD
OGD+exos
OGD+exos+ miR-let-7i-5p inhibitor
OGD+exos+ miR-let-7i-5p inhibitor NC
C
control
OGD
OGD+exos
OGD+exos+miR-let-7i-5p inhibitor
OGD+exos+miR-let-7i-5p inhibitor NC
D
Tunel
DAPI
Merge
100 um
E
Apoptotic rate(%)
F
TUNEL-Apoptosis index
G
Bax
Bcl-2
β-actin
H
Bax Retative pritein expression (β-Actin adjusted)
I
Bcl-2 Retative pritein expression (β-Actin adjusted)

Figure 2. BMSCs-exosomes inhibited hypoxia-induced apoptosis of H9C2 cells through upregulating miRNA-let-7i-5p. (A) CCK-8 assay showed OD values of hypoxic H9C2 cells treated with different concentrations of exosomes (n=6/group). (B) CCK-8 assay showed OD value of hypoxic H9C2 cells treated with exosomes or exosomes transfected with miRNA-let-7i-5p inhibitors (n=6/group). (C) Apoptosis rate was detected by flow cytometry after Annexin V-FITC/PI staining. (D) Apoptotic H9C2 cells detected by TUNEL staining. Scale bar-100 nm. (E) Statistical results of (C) (n=6/group). (F) Statistical results of (D) (n=6/group). (G) Western blot analyses of Bax and Bcl-2 in each group. (H, I) Statistical results of (G), expression of protein levels of Bax (H) and Bcl-2 (I) (n=6/group). *P<0.05. Data are presented as mean ± SEM. BMSCs: Bone marrow mesenchymal stem cells.

Further results showed that the cell survival rate in the OGD group was lower than in the control group. However, treatment with exosomes significantly increased cardiomyocyte survival after OGD treatment compared to the OGD alone group. A similar increase in survival was observed in the miR-let-7i-5p inhibitor NC group. However, the protective effect of exosomes was reversed when the cells were treated with miRNA-let-7i-5p inhibitor (all P<0.05, **Figure 2B**). These findings indicate that BMSCs-exosomes protected H9C2 cell survival through miRNA-let-7i-5p.

BMSCs-exosomes inhibited apoptosis of H9C2 cells after hypoxia by upregulating miRNA-let-7i-5p

Coculture with BMSCs-exosomes partially protected H9C2 cells from OGD-induced cell death. This was further supported by the V-FITC/PI apoptotic assay results (**Figure 2C**). Compared to the control group, OGD significantly increased early and late apoptosis in cardiomyocytes. The OGD-induced injury was significantly mitigated in cells co-cultured with BMSCs-exosomes. As shown in **Figure 2E**, both the OGD+exos group or OGD+exos+miR-let-7i-5p inhibitor NC group exhibited significantly reduced early and late apoptosis compared to the OGD group. In contrast, increased apoptotic rates were observed in the cardiomyocytes treated with OGD alone or OGD+exos+miR-let-7i-5p inhibitor group (all P<0.05).

The same conclusion was confirmed by TUNEL assay. The micrographs showed an increased number of TUNEL-positive myocytes due to hypoxia, which was abated in cells co-treated with BMSCs-exosomes (**Figure 2D**). In comparison with OGD+exos+miR-let-7i-5p inhibitor group, cell apoptosis rate in the OGD+exos group was suppressed. The apoptosis rate in the miR-let-7i-5p inhibitor group was also higher than that in the miR-let-7i-5p inhibitor NC group (all P<0.05, **Figure 2F**). These results suggest that BMSCs-exosomes can inhibit hypoxic-induced apoptosis in H9C2 cells through the upregulation of miRNA-let-7i-5p.

In addition, western blot analysis indicated that Bax expression was lower in the exos group compared to the OGD group and the exos+miR-let-7i-5p inhibitor group (**Figure 2G**). No significant differences in Bax expressions were observed between the OGD group and the miR-Let-7i-5p inhibitor group (all P>0.05, **Figure 2H**). The expression of Bcl-2 was opposite to that of Bax in each group (all P>0.05, **Figure 2I**), suggesting that BMSCs-exosomes inhibited expressions of pro-apoptotic proteins to protect H9C2 cells through miRNA-let-7i-5p.

BMSCs-exosomes reduced infarcted area and improved myocardial function in MI mice by upregulating miRNA-let-7i-5p

The expression of miRNA-let-7i-5p was compared across different groups. RT-qPCR data demonstrated that the relative expression of miRNA-let-7i-5p in the Sham and exos groups was significantly higher than that in the MI group. Compared to the exos group, the expression level of miRNA-let-7i-5p in the miR-let-7i-5p inhibitor group was significantly decreased. Additionally, the miRNA-let-7i-5p expression in the miR-let-7i-5p inhibitor NC group was increased when compared to the miR-let-7i-5p inhibitor group (all P<0.05, **Figure 3A**).

TTC staining indicated that compared to the MI group, a significantly smaller myocardial infarction area was observed in mice myocardial tissues of the Sham group and exos group (**Figure 3B**). However, the infarct size was significantly larger in the miR-let-7i-5p inhibitor group compared to the exos group. Moreover, the infarct size was notably smaller in the miR-let-7i-5p inhibitor NC group than in the miR-let-7i-5p inhibitor group (all P<0.05, **Figure 3C**). These findings suggest that BMSCs-exosomes can

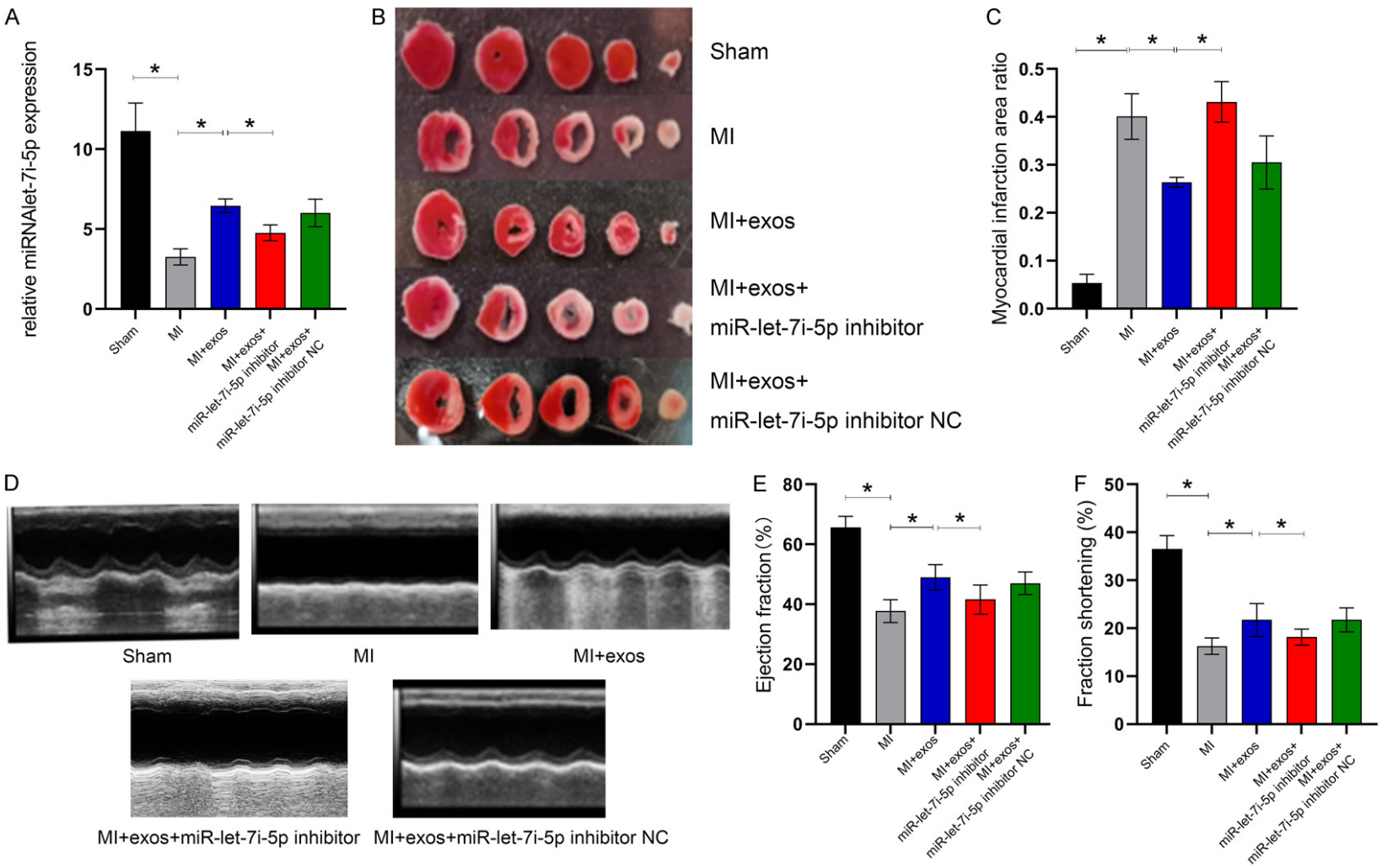

Figure 3. BMSCs-exosomes reduced infarcted area and improved myocardial function in MI mice by upregulating miRNA-let-7i-5p. (A) Relative expression of miRNA-let-7i-5p in infarct myocardium after injecting exosomes or exosomes transfected with miRNA-let-7i-5p inhibitors (n=6/group). (B) TTC staining showed the effect of exosomes or exosomes transfected with miRNA-let-7i-5p inhibitors on infarct size of myocardial tissues in mice. (C) Statistical results of (B), myocardial infraction area ratio (n=6/group). (D) Representative photographs of M-mode echocardiography. (E) Statistical results of (D); LVEF (E) and LVFS (F) (n=6/group). *P<0.05. Data are presented as mean ± SEM. BMSCs: Bone marrow mesenchymal stem cells; LVEF: Left ventricular ejection fraction; LVFS: Left ventricular fractional shortening.

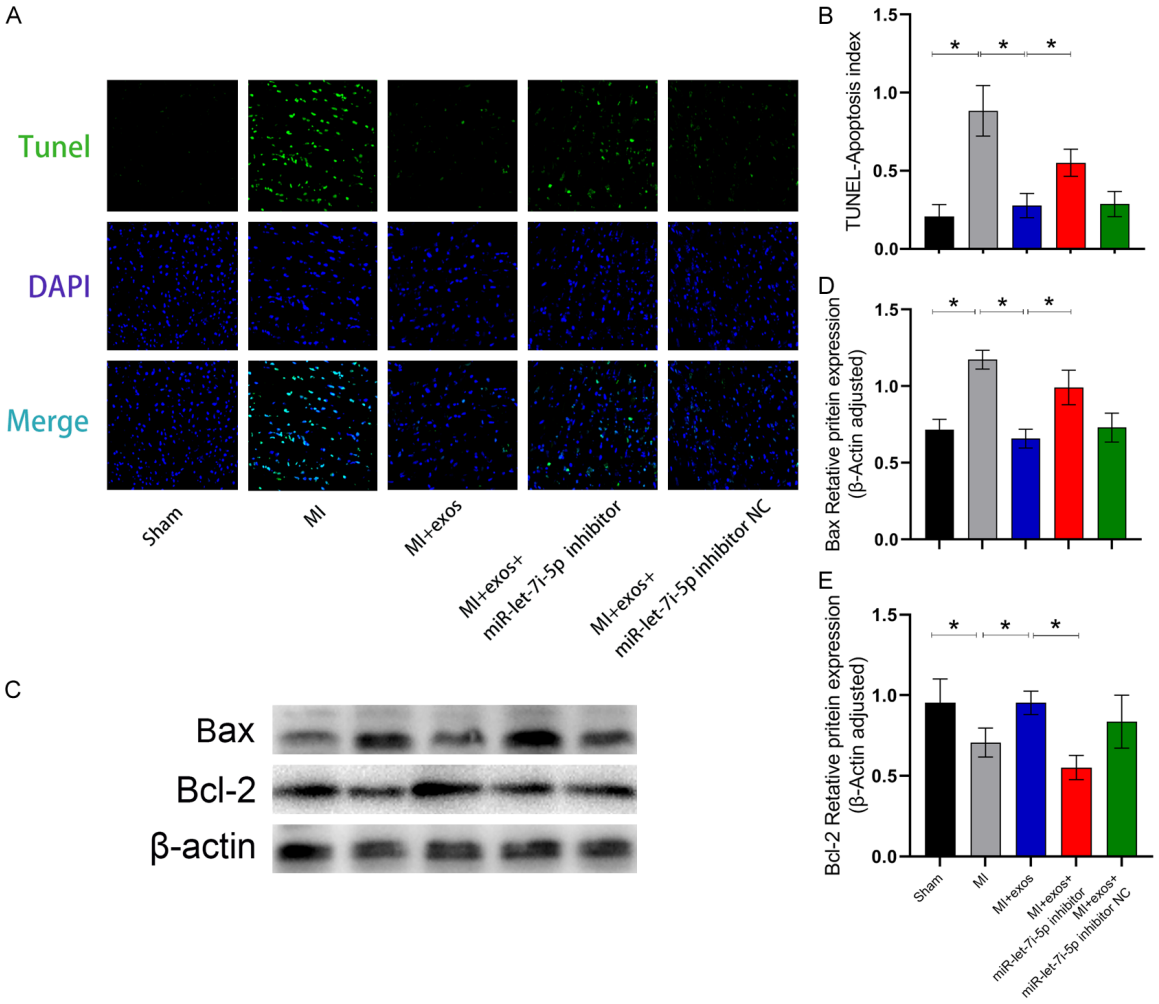

Figure 4. BMSCs-exosomes inhibited cardiomyocyte apoptosis after MI by upregulating miRNA-let-7i-5p. (A) Cell apoptosis index of cardiomyocytes was detected by TUNEL staining. Scale bar-100 nm. (B) Statistical results of (A), apoptosis index (n=6/group). (C) Western blot analyses of Bax and Bcl-2 in each group. (D, E) Statistical results of (C); Protein expression of Bax (D) and Bcl-2 (E) (n=6/group). *P<0.05. Data are presented as mean ± SEM. BMSCs: Bone marrow mesenchymal stem cells.

significantly reduce myocardial infarction area through miRNA-let-7i-5p.

In addition, we examined the effect of exosomal miRNA-let-7i-5p on cardiac function in MI mice (**Figure 3D**). Compared to the Sham group, much lower left ventricular ejection fraction (LVEF) and left ventricular shortening fraction (LVFS) were found in mice of the MI group, exos group, and miR-let-7i-5p inhibitor group. However, the exos group exhibited markedly higher LVEF and LVFS when compared with MI group. Furthermore, LVEF and LVFS were notably lower in the miR-let-7i-5p inhibitor group compared to the exos group (all P<0.05, **Figure 3E**, **3F**). These results indicate that miRNA-let-7i-5p in exosomes secreted by BMSCs contributes to improved cardiac function in mice with MI.

BMSCs-exosomes inhibited cardiomyocyte apoptosis after MI by upregulating miRNA-let-7i-5p

TUNEL results showed that the number of TUNEL-positive myocytes was increased following myocardial infarction (**Figure 4A**). Compared to the MI group, the number of positive myocytes was significantly reduced in the Sham and exos groups. Compared to the miR-let-7i-5p inhibitor group, the number of positive myocytes was significantly lower than that of exos

group and miR-let-7i-5p inhibitor NC group (all P<0.05, **Figure 4B**). Western blot analysis (**Figure 4C**) showed that, compared to the Sham group, the MI group exhibited significantly higher Bax protein expression and significantly lower Bcl-2 protein expression. In addition, the Bcl-2 expression was significantly lower and the Bax expression was obviously higher in myocardial tissues of the MI group compared with exos group. More importantly, compared to the exos group, the miR-let-7i-5p inhibitor group displayed significantly lower Bcl-2 and higher Bax protein expression (all P<0.05, **Figure 4D**, **4E**). These findings suggest that BMSCs-exosomes inhibit cardiomyocyte apoptosis after myocardial infarction through miRNA-let-7i-5p.

Discussion

In recent years, with the increasing prevalence and mortality of coronary atherosclerotic heart disease (CHD), the roles of exosomes on cardiomyocytes have been extensively studied, especially in myocardial infarction (MI). Numerous studies showed that exosomes secreted by mesenchymal stem cells (MSCs) can reduce myocardial infarction area, promote angiogenesis, reduce inflammation, and improve cardiac function [16-18]. MSCs-exosomes are rich in cytokines, phospholipids, ribonucleic acid (RNA) and proteins enabling them to play a crucial role in the pathophysiologic regulation of the cardiovascular system. In addition to MSCs-exosomes, exosomes secreted from other sources also affect CHD [19]. Different cytoprotective factors may exert various protective effects. Among these factors, the role of miRNA contained in exosomes is particularly important. Studies have confirmed that miRNA regulates vascular smooth muscle cells, vascular endothelial cells, myocardial cells and inflammatory cells. Moreover, miRNAs reduce myocardial infarction size, reduce myocardial cell apoptosis, inhibit myocardial fibrosis, suppress ventricular remodeling, and promote angiogenesis, thereby improving cardiac function after MI [20-23]. Let-7 family has been shown to play key roles in heart hypertrophy, cardiac fibrosis, MI, heart failure, dilated cardiomyopathy, angiogenesis, and atherosclerosis [24]. Zhang et al. found that hypoxic cardiomyocyte H9C2 cells could induce the secretion of exosomes containing miRNA-let-7i-5p, which had potential anti-apoptotic and pro-survival effects under hypoxic stress [25]. However, Hu et al. pointed out that the suppression of miRNA-let-7i-5p significantly promoted cardiomyocyte proliferation and improved cardiac function [26].

We established the hypoxia cardiomyocytes by glucose-free DMEM and an MI model in mice by LAD ligation, followed by the injection of BMSCs-exosomes or BMSCs-exosomes transfected with miRNA-let-7i-5p inhibitors in each group. First, we observed that exosomes-miRNA-let-7i-5p improved the survival rate of hypoxic cardiomyocytes, with cell survival rate positively correlated with exosome concentration. Second, *in vivo* experiments showed that miRNA-let-7i-5p expression in the infarcted area decreased after the coronary artery ligation but increased after BMSCs-exosome injection, indicating that BMSCs-exosomes are rich in miRNA-let-7i-5p. Then, exosomes-miRNA-let-7i-5p reduced the infarcted size and improved mice myocardial function in mice.

To investigate whether the up-regulation of miRNA-let-7i-5p contributes to the protective effect of BMSCs-exosomes on cardiomyocytes through anti-apoptosis, we conducted TUNEL, Annexin V-FITC/PI and western blot assays in both *in vivo* and *in vitro* experiments. The results confirmed the anti-apoptotic effect of BMSCs-exosomes-miRNA-let-7i-5p. A limitation of this study is that we did not explore the concrete mechanism by which miRNA-let-7i-5p exerts its anti-apoptotic effect in MI. Our results, however, revealed that BMSCs-exosomes significantly inhibit the apoptosis of cardiomyocytes, attenuate MI progression, and protect myocardial infarction by upregulating miRNA-let-7i-5p expression. Further investigation is needed to determine whether BMSCs-exosomes protect infarcted cardiomyocytes through additional mechanisms, and to clarify the precise pathways involved. Notably, the innovative aspect of this study lies in the experimental injection of BMSCs-exosomes and BMSCs-exosomes transfected with miRNA-let-7i-5p inhibitors into the peri-infarction myocardial region, ensuring their effectiveness.

In conclusion, our study shows that BMSCs-exosomes represent a promising therapeutic modality for MI, offering new insight into MI treatment and providing a rationale for the

development of new therapeutic approaches and techniques. Investigation on the relationship between miRNA-let-7i-5p from BMSCs-exosomes and apoptosis in myocardial infarction is essential to advance our understanding for preventing and treating MI in clinical practice.

Disclosure of conflict of interest

None.

Address correspondence to: Yuanyuan Hao, Department of Cardiology, Xi'an Central Hospital, No. 161 Xiwu Road, Xincheng District, Xi'an 710004, Shaanxi, China. Tel: +86-02984772650; E-mail: hao198155@163.com

References

[1] Pirillo A and Norata GD. The burden of hypercholesterolemia and ischemic heart disease in an ageing world. Pharmacol Res 2023; 193: 106814.

[2] Roth GA, Mensah GA, Johnson CO, Addolorato G, Ammirati E, Baddour LM, Barengo NC, Beaton AZ, Benjamin EJ, Benziger CP, Bonny A, Brauer M, Brodmann M, Cahill TJ, Carapetis J, Catapano AL, Chugh SS, Cooper LT, Coresh J, Criqui M, DeCleene N, Eagle KA, Emmons-Bell S, Feigin VL, Fernández-Solà J, Fowkes G, Gakidou E, Grundy SM, He FJ, Howard G, Hu F, Inker L, Karthikeyan G, Kassebaum N, Koroshetz W, Lavie C, Lloyd-Jones D, Lu HS, Mirijello A, Temesgen AM, Mokdad A, Moran AE, Muntner P, Narula J, Neal B, Ntsekhe M, Moraes de Oliveira G, Otto C, Owolabi M, Pratt M, Rajagopalan S, Reitsma M, Ribeiro ALP, Rigotti N, Rodgers A, Sable C, Shakil S, Sliwa-Hahnle K, Stark B, Sundström J, Timpel P, Tleyjeh IM, Valgimigli M, Vos T, Whelton PK, Yacoub M, Zuhlke L, Murray C and Fuster V; GBD-NHLBI-JACC Global Burden of Cardiovascular Diseases Writing Group. Global burden of cardiovascular diseases and risk factors, 1990-2019: update from the GBD 2019 study. J Am Coll Cardiol 2020; 76: 2982-3021.

[3] Sharma S and Sharma U. Exosomes in cardiovascular diseases: a blessing or a sin for the mankind. Mol Cell Biochem 2022; 477: 833-847.

[4] Li Z, Liu C, Li S, Li T, Li Y, Wang N, Bao X, Xue P and Liu S. BMSC-derived exosomes inhibit dexamethasone-induced muscle atrophy via the miR-486-5p/Fox01 axis. Front Endocrinol (Lausanne) 2021; 12: 681267.

[5] He C, Zheng S, Luo Y and Wang B. Exosome theranostics: biology and translational medicine. Theranostics 2018; 8: 237-255.

[6] Wei Z, Qiao S, Zhao J, Liu Y, Li Q, Wei Z, Dai Q, Kang L and Xu B. miRNA-181a over-expression in mesenchymal stem cell-derived exosomes influenced inflammatory response after myocardial ischemia-reperfusion injury. Life Sci 2019; 232: 116632.

[7] Dai Y, Wang S, Chang S, Ren D, Shali S, Li C, Yang H, Huang Z and Ge J. M2 macrophage-derived exosomes carry microRNA-148a to alleviate myocardial ischemia/reperfusion injury via inhibiting TXNIP and the TLR4/NF-κB/NLRP3 inflammasome signaling pathway. J Mol Cell Cardiol 2020; 142: 65-79.

[8] Chen Q, Liu Y, Ding X, Li Q, Qiu F, Wang M, Shen Z, Zheng H and Fu G. Bone marrow mesenchymal stem cell-secreted exosomes carrying microRNA-125b protect against myocardial ischemia reperfusion injury via targeting SIRT7. Mol Cell Biochem 2020; 465: 103-114.

[9] Bavelloni A, Ramazzotti G, Poli A, Piazzi M, Focaccia E, Blalock W and Faenza I. MiRNA-210: a current overview. Anticancer Res 2017; 37: 6511-6521.

[10] Thomas JJ, Harp KO, Bashi A, Hood JL, Botchway F, Wilson MD, Thompson WE, Stiles JK and Driss A. MiR-451a and let-7i-5p loaded extracellular vesicles attenuate heme-induced inflammation in hiPSC-derived endothelial cells. Front Immunol 2022; 13: 1082414.

[11] Liu Y, Hu X, Hu L, Xu C and Liang X. Let-7i-5p enhances cell proliferation, migration and invasion of ccRCC by targeting HABP4. BMC Urol 2021; 21: 49.

[12] Zhang H, Zou X and Liu F. Silencing TTTY15 mitigates hypoxia-induced mitochondrial energy metabolism dysfunction and cardiomyocytes apoptosis via TTTY15/let-7i-5p and TLR3/NF-κB pathways. Cell Signal 2020; 76: 109779.

[13] Jia J, Zhao XA, Tao SM, Wang JW, Zhang RL, Dai HL, Zhang XJ, Han MH, Yang B, Li Y and Li JT. Icariin improves cardiac function and remodeling via the TGF-β1/Smad signaling pathway in rats following myocardial infarction. Eur J Med Res 2023; 28: 607.

[14] Han BJ, Cao GY, Jia LY, Zheng G, Zhang L, Sheng P, Xie JZ and Zhang CF. Cardioprotective effects of tetrahydropalmatine on acute myocardial infarction in rats. Am J Chin Med 2022; 50: 1887-1904.

[15] Cano A, Ettcheto M, Bernuz M, Puerta R, Esteban de Antonio E, Sánchez-López E, Souto EB, Camins A, Martí M, Pividori MI, Boada M and Ruiz A. Extracellular vesicles, the emerging mirrors of brain physiopathology. Int J Biol Sci 2023; 19: 721-743.

[16] Zhu W, Sun L, Zhao P, Liu Y, Zhang J, Zhang Y, Hong Y, Zhu Y, Lu Y, Zhao W, Chen X and Zhang F. Macrophage migration inhibitory factor facilitates the therapeutic efficacy of mesenchy-

mal stem cells derived exosomes in acute myocardial infarction through upregulating miR-133a-3p. J Nanobiotechnology 2021; 19: 61.
[17] Zhao J, Li X, Hu J, Chen F, Qiao S, Sun X, Gao L, Xie J and Xu B. Mesenchymal stromal cell-derived exosomes attenuate myocardial ischaemia-reperfusion injury through miR-182-regulated macrophage polarization. Cardiovasc Res 2019; 115: 1205-1216.
[18] Sun J, Shen H, Shao L, Teng X, Chen Y, Liu X, Yang Z and Shen Z. HIF-1α overexpression in mesenchymal stem cell-derived exosomes mediates cardioprotection in myocardial infarction by enhanced angiogenesis. Stem Cell Res Ther 2020; 11: 373.
[19] Tong X, Dang X, Liu D, Wang N, Li M, Han J, Zhao J, Wang Y, Huang M, Yang Y, Yang Y, Wang W, Kou Y and Kou J. Exosome-derived circ_0001785 delays atherogenesis through the ceRNA network mechanism of miR-513a-5p/TGFBR3. J Nanobiotechnology 2023; 21: 362.
[20] Xiao Y, Zhao J, Tuazon JP, Borlongan CV and Yu G. MicroRNA-133a and myocardial infarction. Cell Transplant 2019; 28: 831-838.
[21] Song R, Dasgupta C, Mulder C and Zhang L. MicroRNA-210 controls mitochondrial metabolism and protects heart function in myocardial infarction. Circulation 2022; 145: 1140-1153.
[22] McCoy MG, Pérez-Cremades D, Belkin N, Peng W, Zhang B, Chen J, Sachan M, Wara AKMK, Zhuang R, Cheng HS and Feinberg MW. A miRNA cassette reprograms smooth muscle cells into endothelial cells. FASEB J 2022; 36: e22239.
[23] Mahesh G and Biswas R. MicroRNA-155: a master regulator of inflammation. J Interferon Cytokine Res 2019; 39: 321-330.
[24] Bao MH, Feng X, Zhang YW, Lou XY, Cheng Y and Zhou HH. Let-7 in cardiovascular diseases, heart development and cardiovascular differentiation from stem cells. Int J Mol Sci 2013; 14: 23086-23102.
[25] Zhang J, Ma J, Long K, Qiu W, Wang Y, Hu Z, Liu C, Luo Y, Jiang A, Jin L, Tang Q, Wang X, Li X and Li M. Overexpression of exosomal cardioprotective miRNAs mitigates hypoxia-induced H9c2 cells apoptosis. Int J Mol Sci 2017; 18: 711.
[26] Hu Y, Jin G, Li B, Chen Y, Zhong L, Chen G, Chen X, Zhong J, Liao W, Liao Y, Wang Y and Bin J. Suppression of miRNA let-7i-5p promotes cardiomyocyte proliferation and repairs heart function post injury by targetting CCND2 and E2F2. Clin Sci (Lond) 2019; 133: 425-441.